JOURNAL OF SOLID STATE CHEMISTRY **109**, 181–186 (1994)

A Novel Defect Pyrochlore: $(Na_{1.08}V^{V}_{0.43}Sb^{III}_{0.14})(Sb^{V}_{2}O_6)O'_{0.84}$. Preparation and Crystal Structure

A. Haddad

Département de Chimie, Faculté des Sciences de Monastir 5000, Monastir, Tunisie

T. Jouini

Département de Chimie, Faculté des Sciences de Tunis Campus Universitaire, 1060, Tunis, Tunisie

A. Verbaere[1] and Y. Piffard

Laboratoire de Chimie des Solides, Institut des Matériaux de Nantes, UMR CNRS 110, Université de Nantes, 2 rue de la Houssinière, F44072, Nantes Cedex 03, France

and

J. C. Jumas

Laboratoire de Physicochimie des Matériaux Solides, URA CNRS D0407, Université Montpellier II, Place E. Bataillon 34095, Montpellier Cedex 5, France

Received December 12, 1992; accepted July 16, 1993

$(Na_{1.08}V^{V}_{0.43}Sb^{III}_{0.14})(Sb^{V}_{2}O_6)O'_{0.84}$ was obtained by a solid state reaction from $NaNO_3$, V_2O_5, and Sb_2O_3, in air. The formula was inferred from chemical analyses, magnetic susceptibility measurements, and ^{121}Sb Mössbauer spectroscopy. It is in very good agreement with the single crystal structure determination. The refinements lead to $R = 0.016$ and $R_W = 0.019$ for 122 independent reflections and 14 variable parameters. The structure consists of a usual $Sb^{V}_{2}O_6$ pyrochlore framework in which sites situated on or near the 16*d* positions are randomly occupied by Na (16*d*), V^{V}, and Sb^{III} (96*g*). O′ oxygen atoms (32*e*) are strongly bonded to the V^{V} atoms, thus forming VO groups within the framework. The VO_5 polyhedra are irregular and share two edges with two $Sb^{V}O_6$ octahedra. The Sb^{III} polyhedron is similar to that previously observed in $(K_{0.51}Sb^{III}_{0.67})(Sb^{V}_{2}O_6)O'_{0.26}$.

INTRODUCTION

In the course of our investigations of the Na–V–Sb–O system, the title compound was identified as a pyrochlore-type oxide containing Na and Sb, and a small amount of V.

Compounds with a defect (and likely similar) pyrochlore structure have already been identified in the M_2O–Sb_2O_3–Sb_2O_5 systems for M = Na (1) (2) and M = K, Tl (3). The sodium antimonates seem to have the pyrochlore structure for Na : Sb atomic ratios less than 2 : 3 (1). For higher ratios, the ilmenite phase $NaSbO_3$ (4) appears (1). From a crystal structure determination, it was shown that, in the potassium (or thallium) antimonates with a defect pyrochlore structure, Sb^{III} occupies a 96*g* position (3).

This paper reports on the preparation and crystal structure determination of a new defect pyrochlore.

PREPARATION

The title phase is obtained from $NaNO_3$, V_2O_5, and Sb_2O_3 in a molar ratio of 6 : 2 : 3. The mixture is ground before heating in air for 160 hr at 850°C. After cooling, the product is washed with boiling water. Two phases are then observed in the solid: the title compound, as numerous greenish octahedral single crystals up to 0.5 mm on an edge, and a black phase which easily forms a suspension in water, thus allowing a separation. The X-ray powder pattern of the phase obtained is of pyrochlore type. The unit-cell parameter was refined from the X-ray powder pattern (STOE/CCS diffractometer); Table 1 gives the crystallographic data.

---

[1] To whom correspondence should be addressed.

0022-4596/94 $6.00

TABLE 1
Crystallographic Data of $(Na_{1.08}\,V_{0.43}\,Sb^{III}_{0.14})(Sb^{V}_{2}O_{6})O'_{0.84}$

Space group	$Fd\bar{3}m$
a parameter (Å)	10.240 (1)
Volume (Å^3)	1073.7
Z	8
μ (MoK_α) (cm^{-1})	117.3
$D_{calc.}$ (g cm^{-3})	5.16

TABLE 2
Experimental Analysis Results and Values Calculated from Composition (1)

Element	Na	V	Sb	O
% $w_{Exp.}$	5.85	5.21	61.53	23.68
% $w_{calc.}$	5.96	5.26	62.52	26.26

COMPOSITION

Qualitative analyses were performed using an electron microprobe, in a JSM35 scanning electron microscope, for several single crystals of the title phase. They indicate that Na, Sb, and V contents are nearly constant in all the crystals.

Quantitative analyses were performed at the Service Central d'Analyse du CNRS (Vernaison, France). The sample consisted of single crystals. They lead to the atomic ratios

$$\mathrm{Sb/Na} = 1.99/1 \quad \text{and} \quad \mathrm{Sb/V} = 4.93/1.$$

The compound is slightly green, suggesting the occurrence of some V^{IV} atoms. Magnetic susceptibility measurements, however, show a diamagnetic behavior, so that the oxidation state of vanadium is mainly V.

The oxidation state of Sb was inferred from ^{121}Sb Mössbauer spectrometry (samples cooled down to 4.2 K; see Fig. 1). The $Sb^{III}:Sb^{V}$ ratio was evaluated from the peak intensities. Previous similar evaluations have shown (3, 5) the validity of the method, the relative error being a few percent. The fit of the Mössbauer spectrum (Fig. 1) leads to 6.7% Sb^{III} and 93.3% Sb^{V}, with two types (at least) of crystallographic sites for Sb^{III}, and one for Sb^{V}.

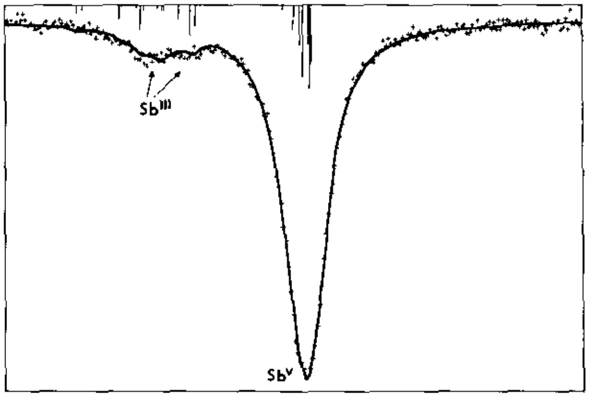

FIG. 1. Experimental and calculated (solid line) ^{121}Sb Mössbauer spectrum of the title phase.

The line associated with Sb^{V} is rather broad, suggesting several similar symmetric sites for Sb^{V}. For Sb^{III}, the two types of sites are very dissymmetric, which suggests a stereochemical activity of the Sb^{III} lone pair.

The results mentioned above lead to the composition

$$Na_{1.08}\,V^{V}_{0.43}\,Sb^{III}_{0.14}\,Sb^{V}_{2}\,O_{6}\,O'_{0.84}. \qquad [1]$$

Table 2 shows good agreement between experimental results and values calculated from composition [1].

CRYSTAL STRUCTURE DETERMINATION

Data Collection

The intensity data were collected from a small crystal (cuboctahedron in shape) with dimensions 0.06 × 0.06 × 0.06 mm^3, using a Nonius CAD4 diffractometer operating under the conditions given in Table 3. On account of the crystal size and of the calculated linear absorption coefficient (μ = 117.3 cm^{-1}) absorption corrections were neglected.

TABLE 3
Collection and Final Refinement Conditions

Collection	
Equipment	Automatic diffractometer Enraf–Nonius CAD4
Radiation (Å)	Mo$K\alpha$, $\lambda = 0.71069$
Scan mode	$\omega - 2\theta$
Scan angle (°)	$\Delta\omega = 1.0 + 0.35 \tan\theta$
Recording angular range (θ°)	1.5–35.0
Number of measured intensities ($\frac{1}{4}$ of reciprocal space)	5196
Refinement	
Number of independent data observed with $\sigma(I)/I < 0.33$ and used in refinements	122
Number of variables	14
$R = \Sigma[\lvert F_o - F_c\rvert]/\Sigma\lvert F_o\rvert$	0.016
$R_w = [\Sigma_w(F_o - F_c)^2/\Sigma F_o^2]^{1/2}$ with $w = 1$	0.019
Extinction parameter refined g	5.95(4) × 10^{-6}

Refinements

For the data reduction and the structure refinements, the SDP-PLUS program chain (1982 version) of Enraf–Nonius (6) was used, taking into account anomalous dispersion and secondary extinction. Strong extinction effects are frequently observed in pyrochlore crystals, and when they cannot be corrected satisfactorily, it is often preferable to remove from the data set one or several strong reflections strongly affected by this phenomenon. In the present case, reflection (440) was used in the preliminary stages of the refinement but removed in the final one.

Owing to the expected structure type and to the composition, the octahedral sites of the pyrochlore structure were first supposed to be mainly occupied by Sb^{V} atoms. In the first step, Sb and O were situated on 16*c* and 48*f* positions of space group $Fd\bar{3}m$, respectively, forming a $Sb^{V}_{2}O_{6}$ pyrochlore octahedral framework. The refinement, including the anisotropic temperature factors, leads to

$$R = 0.076, \qquad R_W = 0.083.$$

The difference Fourier map then shows a significant peak in the 16*d* position, which is quite convenient for the Na^{+} ions. Accordingly, Na was introduced in 16*d* (with an isotropic temperature factor), with a fixed occupancy of 53.9%, in agreement with composition [1]. This second step leads to

$$R = 0.044, \qquad R_W = 0.051,$$

and in the difference Fourier map two weak peaks (nearly 1 e Å^{-3}, other peaks being much weaker) are observed:

(i) in the 96*g* position, 0.6 Å from 16*d* (possible position for V^{V} and/or Sb^{III})

(ii) in the 32*e* position, 0.8 Å from 8*b* (possible position for extra oxygen atoms O′).

It can be emphasized that no maxima are observed in 8*b* positions, and that the *R* factors increase when oxygen atoms are introduced in this site.

Two types of positions could be considered as possible for V^{V} atoms:

(i) 16*c*, as $(Sb^{V}_{2-x}V^{V}_{x})$,

(ii) a 96*g* position as mentioned above.

The refinements performed for (i) do not lower the *R* factors, whereas an important lowering is observed for (ii), which makes this option more likely.

TABLE 4
Fractional Atomic Coordinates and Thermal Parameters
B^{*} or B_{eq} (Å^2)

Atom	Position	Number per unit cell	x/a	y/a	z/a	B^{*} or B_{eq}
Sb^{V}	16*c*	16	0	0	0	0.599(1)
Na	16*d*	8.63	½	½	½	1.42(9)*
V^{V}	96*g*	3.48	0.5255(9)	x/a	0.436(1)	0.7(2)*
Sb^{III}	96*g*	1.15	0.5125	x/a	0.462	2*
O	48*f*	48	0.3231(3)	⅛	⅛	1.32(3)
O′	32*e*	6.73	0.419(1)	x/a	x/a	1.8(4)*

Note. $B_{eq} = \frac{4}{3}\Sigma_i\Sigma_j\,\beta_{ij}a_ia_j$.

In a third step, V and O′ were then introduced in 96*g* and 32*e* positions, respectively, as mentioned above, and numerous refinements were performed for various fixed values of the V and O′ occupancies. The best result corresponds to $R = 0.017$, $R_W = 0.020$, and to the composition

$$(Na_{1.23}V^{V}_{0.62})(Sb^{V}_{2}O_{6})O'_{0.84}. \qquad [2]$$

This composition (nonneutral) has of course nothing to do with the actual one since it does not take the Sb^{III} content into account. However, one can mention that:

(i) the oxygen content is confirmed

(ii) Na and V contents slightly higher than those expected (composition 1) strongly suggest that Sb^{III} occupies a 96*g* position also close to 16*d*, and probably between the Na and V positions.

As a matter of fact, in $(K_{0.51}Sb^{III}_{0.67})(Sb^{V}_{2}O_{6})O'_{0.26}$, Sb^{III} is in a 96*g* position (3) extremely close to the midpoint between our Na and V positions. Consequently, in the final refinements, the position retained and fixed for Sb^{III} was that given in Ref. (3).

Because of strong correlations and of the number of independent data, the positional, thermal, and occupancy parameters of Na, V, and Sb^{III} atoms cannot be simultaneously refined. Accordingly, various refinements were performed with selected fixed parameters in turn, in order to check the model obtained, and then, in the final refinement, the following parameters were fixed:

(i) all the occupancies (according to composition [1],

(ii) all the parameters for Sb^{III}.

The results are given in Tables 3–5. The maxima of the

TABLE 5
Anisotropic Temperature Factors (Å^2 × 10^3)

Atom	U_{11}	U_{22}	U_{33}	U_{12}	U_{13}	U_{23}
Sb^{V}	7.58(6)	U_{11}	U_{11}	−2.05(8)	U_{12}	U_{12}
O	14(1)	18.2(7)	U_{22}	0	0	11(1)

Note. The form of the anisotropic thermal factor is $\exp[-2\pi^2(h^2a^{*2}U_{11} + k^2b^{*2}U_{22} + l^2c^{*2}U_{33} + 2hka^{*}b^{*}U_{12} + 2hla^{*}c^{*}U_{13} + 2klb^{*}c^{*}U_{23})]$.

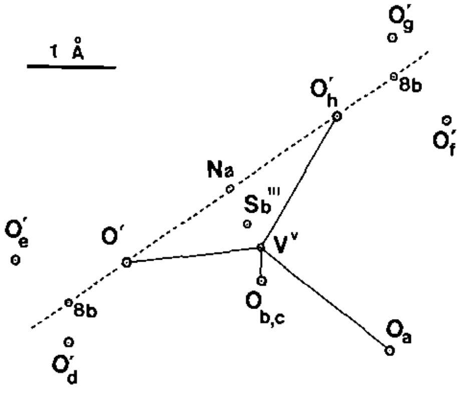

FIG. 2. Schematic representation of the cation environments in an *A*-site. Equivalent positions of Sb^{III} and V^V are not shown. All atoms, except $O_{b,c}$, O'_d, and O'_g, lie in the figure plane (i.e., a mirror plane). The broken line is along [111], and solid lines show the V bonding.

final difference Fourier map are in the range ±0.3 e Å^{-3}. (Structure factor table will be sent upon request.)

DESCRIPTION AND DISCUSSION OF THE STRUCTURE

The structure of $(Na_{1.08}\ V_{0.43}\ Sb^{III}_{0.14})(Sb^V_2O_6)O'_{0.84}$ exhibits a $Sb^V_2O_6$ pyrochlore framework. Such a framework delimits large cavities which intercommunicate via hexagonal windows. Each cavity and each window is centered on a 8*b* and a 16*d* position, respectively. Let us call the vicinity (or the center) of these two positions *X*- and *A*-sites, respectively. A full occupancy of the *X*- and *A*-sites in a B_2O_6 framework leads to the well-known $A_2B_2O_6X$ formula; numerous examples of compounds exist for which *A* is a cation and *X* an oxygen ion (2).

In the title compound, Na, V^V, and Sb^{III} atoms are randomly distributed over the *A*-sites, which are occupied at 82.8% (53.9% by Na, 21.7% by V^V, and 7.2% by Sb^{III}). The O′ extra oxygen atoms are on *X*-sites, with an occupancy of 84%. Since the O′–8*b* distance is 0.78 Å, a *X*-site cannot be occupied by more than one O′ atom. Figure 2 shows atomic positions in an *A*-site and two adjacent *X*-sites. On account of the ionic radii (8) and calculated interatomic distances, simultaneous occupancy of some sites are precluded.

With Na or Sb^{III} on a given site (16*d* or 96*g*, respectively), the two closest 32*e* sites, O′ and O'_h (see Fig. 2), must be empty. Other O′ sites may be filled as mentioned above, so that the number of O′ neighbors for Na and Sb^{III} is 0, 1, or 2.

Table 6 presents selected interatomic distances and angles with the highest possible coordinations in the case of Na, Sb^{III}, and V^V. The symmetry code used in this table agrees with the symbols in Fig. 2. Figure 3 gives illustrations of such coordinations, which are in good agreement with previous knowledge of Na, Sb^{III}, Sb^V, and V^V crystal chemistry, and with the ionic radii (8). Table 7 gives the X-ray powder diffraction data.

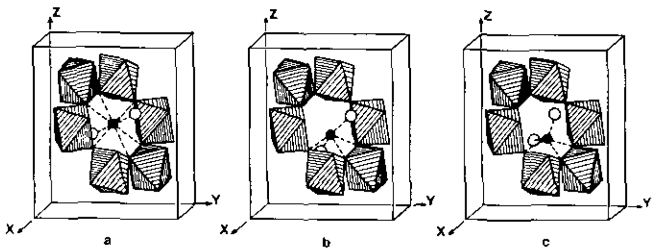

FIG. 3. Views of part of the unit cell centered on an *A*-site, showing a hexagonal window in the framework. Open circles represent O′ atoms and closed circles represent Na (a), Sb^{III} (b), and V^V (c).

It is interesting to briefly discuss the Sb and V environments, taking into account the rather high O′ occupancy of the *X*-site, and the main features of the ^{121}Sb Mössbauer spectra. In the case of Sb^{III}, the two different dissymmetric sites inferred from these spectra can be associated to the occurrence of mainly two environments (3O + O′ and 3O + 2O′), which are very dissymmetric. For Sb^V, the nearest neighbors form a rather regular octahedron, and the occurrence of Sb^{III} or V^V as next nearest neighbors of some Sb^V atoms explains the width of the Sb^V line in the spectra. In the case of V^V, a very dissymmetric polyhedron VO_3 or VO_4, with the O′ and/or O'_h sites (see

TABLE 6

Selected Interatomic Distances (Å) and Bond Angles (°) in $(Na_{1.08}\ V^V_{0.43}\ Sb^{III}_{0.14})(Sb^V_2O_6)O'_{0.84}$

Sb^VO_6 octahedron			
Sb^V–O	1.964 (1) (6x)	O–Sb^V–O	94.2 (1) 85.8 (1)
NaO_8 polyhedron			
Na–O	2.567 (2) (6x)	Na–O'_f or O'_g	2.58 (1)
Na–O'_d or O'_e	2.58 (1)	O–Na–O	62.79 (2)
$Sb^{III}O_5$ polyhedron			
Sb^{III}–O_a	2.168	Sb^{III}–O'_d (or O'_e)	2.49 (or 2.66)
Sb^{III}–$O_{b,c}$	2.374 (2x)	Sb^{III}–O'_f (or O'_g)	2.58 (or 2.75)
VO_5 polyhedron			
V–O′	1.56 (1)	O′–V–O'_h	125.2 (6)
V–O'_h	1.69 (1)	O′–V–O_a	134.6 (7)
V–O_a	1.85 (1)	O′–V–$O_{b,c}$	88.3 (3) (2x)
V–$O_{b,c}$	2.27 (1) (2x)	O'_h–V–O_a	100.2 (3)
		O'_h–V–$O_{b,c}$	103.9 (3) (2x)
		O_a–V–$O_{b,c}$	80.0 (3) (2x)
		O_b–V–O_c	148.0 (6)

Symmetry code:

a: $\frac{5}{8}, \frac{5}{8}, x$	b: $1-x, \frac{3}{8}, \frac{3}{8}$	c: $\frac{3}{8}, 1-x, \frac{3}{8}$
d: $x, \frac{3}{4}-x, \frac{3}{4}-x$	e: $\frac{3}{4}-x, \frac{3}{4}-x, x$	f: $\frac{1}{4}+x, \frac{1}{4}+x, 1-x$
g: $1-x, \frac{1}{4}+x, \frac{1}{4}+x$	h: $1-x, 1-x, 1-x$	

Note. See text and fig. 2.

TABLE 7
X-Ray Powder Diffraction Data of the Title Phase

h	*k*	*l*	d_{calc} (Å)	d_{obs} (Å)	I/I_o[1]
1	1	1	5.9121	5.9268	71
3	1	1	3.0875	3.0890	39
2	2	2	2.9561	2.9573	100
4	0	0	2.5600	2.5605	26
3	3	1	2.3492	2.3476	7
3	3	3	1.9707	1.9702	15
5	1	1			
4	4	0	1.8102	1.8096	44
5	3	1	1.7309	1.7300	17
5	3	3	1.5616	1.5609	7
6	2	2	1.5438	1.5430	38
4	4	4	1.4780	1.4774	10
5	5	1	1.4339	1.4335	14
7	1	1			
7	3	1	1.3331	1.3329	14
5	5	3			
8	0	0	1.2800	1.2800	7
7	3	3	1.2510	—	2
6	6	0	1.2068	—	1
8	2	2			
5	5	5	1.1824	1.1827	6
7	5	1			
6	6	2	1.1746	1.1749	20
8	4	0	1.1449	1.1452	18
7	5	3	1.1240	1.1245	10
9	1	1			

Note. Intensities less than 1 are not given.

[1] Intensities calculated using the Lazy-Pulverix program (7).

Fig. 2) empty, is hardly credible, so that the coordination of V^{V} must correspond to the VO_5 irregular polyhedron described by Figs. 2 and 3, and Table 6. The shortest bond length, 1.56(1) Å, is very close to those observed in α- and β-$VOPO_4$ (9, 10), and in $Tl_{0.48}V_2O_5$ (11). The longest ones correspond to oxygen atoms bonded to Sb^{V}, with low O–V–O angle values. These features may be related to the fact that the VO_5 polyhedron shares two of its edges with two $Sb^{V}O_6$ octahedra (Fig. 3), and to the V^{V}–Sb^{V} repulsion. The results obtained for the V^{V} polyhedron imply two filled O′ sites for each occupied V site, as in Fig. 2. For 0.43 V in the title formula, the O′ content should then be 0.86, in fair agreement with the experimental value.

Finally, it can be noticed that, for V in a given *A*-site, the neighboring *A*-sites can be occupied by Na or Sb^{III} (or nothing), but not by other V atoms.

In order to provide support for the structural results concerning the V and O′ atoms, Raman spectra were recorded in the 1200–360 cm^{-1} range, using a single crystal and a MICRODIL 28 spectrometer (incident beam not polarized, Spectra Physics 2000 argon ion laser). The few emission bands observed in the 750–400 cm^{-1} range are mainly associated with the Sb–O bonding and O–V–O bending, and some of them are broad, which is possibly due to local perturbations of the Sb–O bonds by cations in the *A*-sites.

At higher energy, from 970 to 800 cm^{-1}, four bands are observed: a strong one at 908 cm^{-1}, with shoulders at 931 and 953 cm^{-1}, and a broad band at 850 cm^{-1}. They must be determined by stretching vibrations of short V–O bonds, since bands from Sb–O stretching are very unlikely at these frequencies, in particular for a regular SbO_6 octahedron.

Raman and infrared data concerning VO_5 polyhedra with short V–O bonds have already been reported. For VO_5 polyhedra with a single short V–O_l bond (associated to a single unshared vertex), the V–O_l stretching vibrations give bands between 1030 and 920 cm^{-1} (12–15), and more particularly Raman spectra show a very strong band between 925 and 970 cm^{-1} (15). For VO_5 polyhedra with two short V–O bonds (two unshared vertices), slightly lower frequencies have been reported: this is the case for $LiVTeO_5$, in which the two short bond lengths are similar (1.66 and 1.72 Å) (16), and the infrared adsorption spectrum then shows bands at 935, 920, and 880 cm^{-1}, corresponding to ν_{VO_2} vibrations (17).

For the title compound, quite similar values are obtained in this frequency domain. The highest energy, however, corresponds to 953 cm^{-1} (instead of 935 cm^{-1} for $LiVTeO_5$), and the lowest to 850 cm^{-1} (instead of 880 cm^{-1}. This difference could well be explained by the difference in the lengths of the two short V–O bonds (1.56 and 1.69 Å, instead of 1.66 and 1.72 Å in $LiVTeO_5$).

In conclusion, this preliminary investigation of the vibrational properties agrees well with the structural results and clearly demonstrates the existence of short V–O bonds. However, it is difficult to predict what would be the V–O bonding and the corresponding vibrations for V in octahedral sites of the framework.

Nevertheless, it has recently been shown that high-pressure conditions are required for the preparation of $Mn^{II}_{2}(V_xSb_{2-x}O_6)O'$ pyrochlore antimonates (18), i.e., to stabilize V^{V} in the octahedral sites of a Sb_2O_6 pyrochlore framework. For the title compound, prepared under normal pressure, the existence of VO groups within the tunnel of the Sb_2O_6 framework appears, then, likely.

CONCLUDING REMARKS

The title compound belongs to the family of defect pyrochlore compounds, as previously reported alkali-antimonates (1–3). For Sb^{III} and Sb^{V}, the bonding is similar to that obtained for instance in $(K_{0.51}\ Sb^{III}_{0.67})\ (Sb^{V}_{2}O_6)\ O'_{0.26}$ (3). The most salient feature of the title compound is the position of V^{V}, which forms an irregular VO_5 polyhedron with a short V–O bond length, as in a VO group. This rather unexpected polyhedron shares two edges with two octahedra of the pyrochlore framework.

REFERENCES

1. D. J. Stewart and O. Knop, *Can. J. Chem.* **48,** 1323 (1970).
2. M. A. Subramanian, G. Aravamudan, and G. V. Subba Roa, *Progr. Solid State Chem.* **15,** 55 (1983).
3. Y. Piffard, M. Dion, and M. Tournoux, *Acta Crystallogr., Sect. B* **34,** 366 (1978); Y. Piffard and M. Tournoux, *Acta Crystallogr., Sect. B.* **35,** 1450 (1979).
4. N. Schrewelius, *Z. Anorg. Allg. Chem.* **238,** 241 (1938).
5. A. Jouanneaux, S. Oyetola, A. Verbaere, D. Guyomard, A. Fitch, and Y. Piffard, *Eur. J. Solid State Inorg. Chem.* **28,** 755 (1991).
6. B. Frenz, "Enraf–Nonius Structure Determination Package." Delft Univ. Press, Delft, Holland, 1982.
7. R. Yvon, W. Jeitschko, and E. Parthe, *J. Appl. Crystallogr.* **10,** 73 (1977).
8. R. D. Shannon, *Acta Crystallogr., Sect. A* **32,** 751 (1976).
9. B. D. Jordan and C. Calvo, *Can. J. Chem.* **51,** 2621 (1973).
10. R. Gopal and C. Calvo, *J. Solid State Chem.* **5,** 432 (1972).
11. M. Ganne, A. Jouanneaux, and M. Tournoux, *J. Solid State Chem.* **97,** 186 (1992).
12. N. G. Chernorukov, N. P. Egorov, and I. A. Korshunov, *Russ. J. Inorg. Chem.* (*Engl. Transl.*) **23,** 1479 (1978).
13. M. Martinez Lara, A. Jimenez Lopez, L. Moreno Real, and S. Bruque, *Mater. Res. Bull.* **20,** 549 (1985).
14. B. Chauvel, P. Bondot, M. De Roy, and J. P. Besse, *Mater. Res. Bull.* **26,** 487 (1991).
15. G. T. Stranford and R. A. Condrate, *Spectrosc. Lett.* **17,** 85 (1984).
16. J. Darriet, *Bull. Soc. Fr. Mineral. Crystallogr.* **96,** 97 (1973).
17. V. Dimitrov, *J. Solid State Chem.* **66,** 256 (1987).
18. M. A. Subramanian, *Mater. Res. Bull.* **27,** 939 (1992).